Journal of Geodesy (2001) 75: 331–336

Journal of Geodesy

An improvement to ionospheric delay correction for single-frequency GPS users – the APR-I scheme

Y. Yuan, J. Ou

Institute of Geodesy and Geophysics, Chinese Academy of Sciences, 54 Xudong Road, Wuhan, 430077, China
e-mail: ojk1009@public.wh.hb.cn; Fax: +86-27-86783841

Received: 24 December 1999 / Accepted 21 February 2001

Abstract. For the commonly used GPS wide-area augmentation systems (WAAS) with a grid ionospheric model, the efficient modelling of ionospheric delays in real time, for single-frequency GPS users, is still a crucial issue which needs further research. This is particularly necessary when differential ionospheric delay corrections cannot be broadcast, when users cannot receive them, or when there are ionospheric anomalies. Ionospheric delays have a severe effect on navigation performance of single-frequency receivers. A new scheme is proposed which can efficiently address the above problems. The robust recurrence technique is based on the efficient combination of single-frequency GPS observations by users and the high-precision differential ionospheric delay corrections from WAAS. Its effectiveness is verified with examples.

Key words: WAAS – APR-I – Ionospheric Delay – Single-frequency GPS Users

1 Introduction

It is difficult to account precisely for the ionospheric delays for single-frequency GPS receivers. In general, the ionospheric correction model broadcast with the GPS signals is inadequate for many GPS users, and its effectiveness will be less under abnormal ionospheric conditions (Klobuchar 1982; Campbell et al. 1986; Henson and Collier 1986; Beutler et al. 1988). Hence, much effort has been invested in this research area (see e.g. Georgiadou and Kleusberg 1988; Goad 1990; Wild et al. 1990; Cohen et al. 1992; Sardon et al. 1994; Qiu et al. 1995; Li and Schwarz 1996; Wang and Wilkinson 1997).

Recently it has been recognized that the wide-area augmentation system (WAAS) with a grid ionospheric model is one of the most effective methods for modelling ionospheric delays for single-frequency users. The WAAS broadcasts its differential ionospheric delay corrections (DIDC) in real time. The DIDCs are vertical ionospheric delay estimates (GVIDE) at each of the ionospheric grid points (IGP) of an ionospheric delay correction grid covering the service area (Conker et al. 1995; Gao et al. 1996; Lin et al. 1996; Wang et al. 1996). The WAAS broadcasts GVIDE values to users approximately once every DUP (data update period, typically 5 minutes) (Conker et al. 1995). Thus, the user receiver can only process the GVIDE obtained at the beginning time t_r of one DUP to calculate the vertical and slant ionospheric delay estimates for each of its ionospheric pierce points (IPP), at any observation epoch t_j during the corresponding DUP (i.e. $t_j \in [t_r, t_r + \mathrm{DUP}]$) (Chao et al. 1995; Conker et al. 1995]. The WAAS's DIDC received by single-frequency GPS receivers can usually correct for the ionospheric delays to observations under normal conditions. However, the ionospheric delays cannot be efficiently accounted for during those periods when the WAAS cannot broadcast DIDC values to users, or when the receivers can not receive the DIDCs for whatever reason. The ionospheric delay corrections will be less well known in cases when the variations of the ionospheric delays may be very large due to ionospheric disturbances (Conker et al. 1995; Pullen et al. 1996; Ho et al. 1997). In the present paper, first the single-frequency observation equation is introduced in Sect. 2. Then in Sect. 3 a new method, based on a robust recurrence procedure and an efficient combination approach (between absolute ionospheric delays and ionospheric relative changes), is introduced. Preliminary experimental results, conclusions and discussions are given in Sects. 4 and 5.

2 Analysis of availability of determining ionospheric delays

If ϕ_1 is the L_1 phase measurement and D_1 is the C/A code measurement, then the single-frequency combination

Correspondence to: Y. Yuan

observation equation can be written as (Georgiadiou 1994; Yuan and Ou 1999)

$$L_{D\phi_1} = D_1 - \phi_1 = 2I_1 + N_{SR1} + \Delta\varepsilon_{D\phi_1} = 2mf \cdot I_{1,v} + N_{SR1} + \Delta\varepsilon_{D\phi_1} \quad (1)$$

where $N_{SR1} = [(S_{D_1} - S_{\phi_1}) + (R_{D_1} - R_{\phi_1}) - N_1]$; $\Delta\varepsilon_{D\phi_1} = \varepsilon_{D_1} - \varepsilon_{\phi_1}$; S and R are the satellite and receiver biases on the corresponding code or phase measurements, respectively; N_1 is the unknown ambiguity for the L_1 phase measurements; $I_{1,v}$ and $I_1 = mf \cdot I_{1,v}$ are the vertical and slant ionospheric delays on the C/A code or L_1 phase measurements, respectively; ε represents observation noises and other random errors; and mf is the ionospheric mapping function (Ou 1996). All quantities in the above equation are expressed in units of length (except for mf).

According to Eq. (1), it is possible to write

$$\Delta I_1(t, t+1) = I_1(t+1) - I_1(t) = \tfrac{1}{2}\left[L_{D\phi_1}(t+1) - L_{D\phi_1}(t)\right] + \tfrac{1}{2}[\Delta\varepsilon(t+1) - \Delta\varepsilon(t)] \quad (2a)$$

where t is the observation epoch; $\Delta I_1(t, t+1)$ is the variation of the ionospheric delay between epoch t and $t+1$; and $L_{D\phi_1}(t) = 2I_1(t) + N_{SR1} + \Delta\varepsilon_{D\phi_1}(t)$. From $\Delta I_1(t, t+1)$ and Eq. (2a), $\nabla I_1(t_j, t_m)$, the variation of the ionospheric delays between two arbitrary epochs t_j and t_m, can be obtained

$$\nabla I_1(t_j, t_m) = \sum_{t=t_j}^{t_{m-1}} [\Delta I_1(t, t+1)] \quad (t_m > t_j) = \tfrac{1}{2}\left[L_{D\phi_1}(t_m) - L_{D\phi_1}(t_j)\right] + \tfrac{1}{2}[\Delta\varepsilon(t_m) - \Delta\varepsilon(t_j)] \quad (2b)$$

If the effects of $\Delta\varepsilon$ are ignored (especially for disturbed ionospheric conditions), then approximate values of $\nabla I_1(t_j, t_m)$ can be estimated

$$\hat{\nabla} I_1(t_j, t_m) = \tfrac{1}{2}\left[L_{D\phi_1}(t_m) - L_{D\phi_1}(t_j)\right] \quad (2c)$$

From Eqs. (1) and (2), it can be seen that it is impossible to determine absolute ionospheric delays in real time using only single-frequency measurements. However, the variation of ionospheric delay can be calculated in real time, assuming that N_{SR1} can be approximated as a constant over several hours. Figures 1 and 2 show changes of ionospheric delay $\hat{\nabla} I_1(t_j, t_m)$ for satellite PRN = 1 under calm conditions, and for satellite PRN = 9 under disturbed ionospheric conditions, respectively. From a comparison of Figs. 1 and 2 it can be seen that $\hat{\nabla} I_1(t_j, t_m)$ will efficiently and directly reflect the ionospheric variations from single-frequency measurements. $\hat{\nabla} I_1(t_j, t_m)$ is relatively stable under calm ionospheric conditions, while it can also efficiently indicate the ionospheric delay changes [which are the major components of $\nabla I_1(t_j, t_m)$] during abnormal ionospheric conditions. Figures 1 and 2 also illustrate that the curves of relative ionospheric delay changes $\hat{\nabla} I_1(t_j, t_m)$ (determined from single-frequency observations) are approximated by the absolute ionospheric delays estimated from dual-frequency GPS observations. The differences are almost a constant, whose magnitude is approximately that of the slant ionospheric delay $I_1(t_j)$ at the initial epoch t_j. Delikaraoglou (1989) also discusses this finding. This shows that if a precise estimate of the initial absolute ionospheric delay can be provided for $\hat{\nabla} I_1(t_j, t_m)$, then the slant ionospheric delay at t_m can be determined with high precision, according to

$$\hat{I}_1(t_m) = I_1(t_j) + \hat{\nabla} I_1(t_j, t_m) = I_1(t_j) + \tfrac{1}{2}\left[L_{D\phi_1}(t_m) - L_{D\phi_1}(t_j)\right] \quad (3)$$

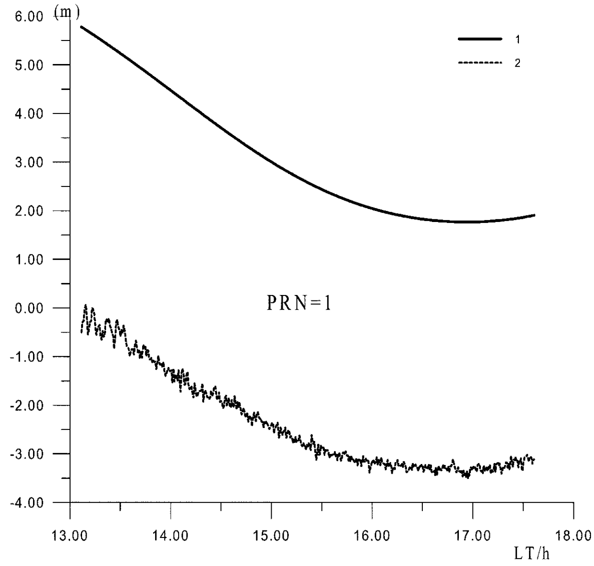

Fig. 1. Comparison of the estimated ionosphere absolute delays and relative variations between observation epoch to initial epoch under calm conditions. *1* The calculated IONs using dual frequency GPS data; *2* the estimated IONs variation using single frequency GPS data

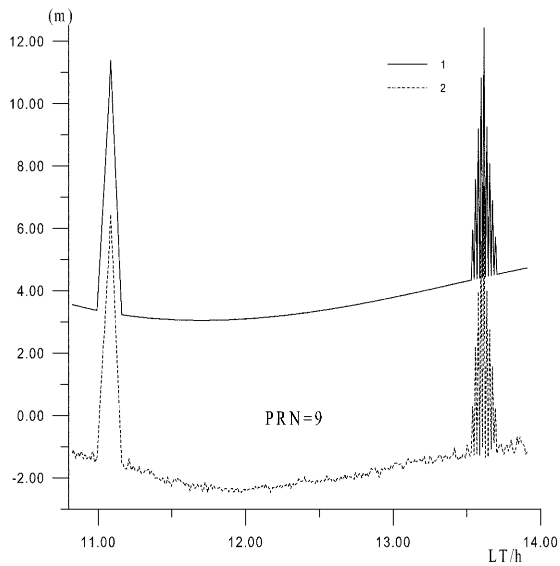

Fig. 2. Comparison of the estimated ionosphere absolute delays and relative variations between observation epoch and initial epoch during short time scale ionospheric disturbances. *1* The calculated IONs using dual frequency GPS data; *2* the estimated IONs variation using single frequency GPS data

3 A new ionospheric delay correction scheme for single-frequency GPS data – the APR-I scheme

Let (t_{er1}, t_{er2}) denote the time period when any or all of the three abnormal conditions referred to above may occur, and t_r the closest DIDC reception epoch [i.e. the closest DIDC transmission time from the WAAS, without considering the travel delay of DIDC (Jin 1995)]. As mentioned earlier, the WAAS can provide high-precision *absolute* ionospheric delay estimates when it operates properly, and a single-frequency GPS receiver can efficiently determine the *relative* variation of ionospheric delay. As a result, if the WAAS cannot broadcast the DIDC, or users cannot receive them, and the ionospheric delay varies more severely than usual, a user serviced by the WAAS may determine the ionospheric delays in real time using the absolute ionospheric delays based on GVIDE (which had been received under normal conditions) and corresponding GPS observations, and real-time single-frequency GPS measurements using the following approach. The proposed approach is referred to as APR (absolute plus relative). APR involves the following procedure.

(1) For the observation epochs outside the period (t_{er1}, t_{er2}), one directly uses the DIDC from the WAAS to obtain the slant ionospheric delay correction.

(2) For the observation epochs inside the period (t_{er1}, t_{er2}), the high-precision DIDC collected and stored during the time period (t_0, t_{er1}) and its corresponding slant ionospheric delay measurements are combined with real-time slant ionospheric delay observations at any epoch $t_m \in (t_{er1}, t_{er2})$. The real-time ionospheric delay corrections are computed according to the following procedure.

(a) *Selecting ideal initial absolute ionospheric delay values*. From $I_1(t_j)$ [calculated using the received DIDC from the q WAAS messages broadcast for the intervals which are closest to epoch t_{er1} during (t_0, t_{er1})], the user selects l vertical ionospheric delay estimates $I_1(t_{ji})$ $(j = 1, 2, \ldots, l,\ l > k$, where l is the number of selected initial computation epochs t_{ji}, and k is the number of necessary initial epochs). Here $t_j \in (t_r - q \cdot \mathrm{DUP}, t_r)$ and $t_r \in (t_{er1} - \mathrm{DUP}, t_{er1})$.

Let t_{ref} (one can select $t_{\mathrm{ref}} = t_r - \mathrm{DUP} \cdot q$) be the reference epoch, and T denote the average length of time period between the initial epochs. Separating the time period (t_{ref}, t_r) into l subsidiary time intervals T_{ik} [where $l = \mathrm{int}(\mathrm{DUP} \cdot q/T)$, and int denotes the operator of rounding to an integer] and then selecting $l_1 t_{ji}$ $(i = 1, 2, \ldots, l_1)$ from one T_{ik} (i.e. $t_{ji} \in [t_{\mathrm{ref}} + (ik - 1) * T,\ t_{\mathrm{ref}} + ik * T]$, $ik = 1, 2, \ldots, l$), one can obtain l l_1 – epoch sets to be used as preselected initial epochs. Thus, according to Eq. (3), one may determine l_1 slant ionospheric delays $\hat{I}_1(t_{\mathrm{ref}})_i$ for reference t_{ref} for one T_{ik}, and then select one epoch t_{ji} [which satisfies the condition of Eq. (4a) below] as the ideal epoch. So, one can obtain l ideal initial epochs (one in a T_{ik}) and refer to them as epoch set DI

$$\left|\hat{I}_1(t_{\mathrm{ref}})_{\substack{ji \\ 1 \le i \le l_1}} - \operatorname*{med}_{1 \le i \le l_1}\left[\hat{I}_1(t_{\mathrm{ref}})_i\right]\right| = \min_{1 \le i \le l_1}\left|\hat{I}_1(t_{\mathrm{ref}})_i - \operatorname*{med}_{1 \le i \le l_1}\left[\hat{I}_1(t_{\mathrm{ref}})_i\right]\right| \quad (4a)$$

where med is the operator for determining the median and min is the operator for determining the minimum. [Details of how to identify the time period (t_{er1}, t_{er2}), and detect/repair cycle slips, and select $(t_r - q \cdot \mathrm{DUP}, t_r)$ from the time period (t_0, t_{er1}) in real time will be discussed in another paper.]

(b) *Calculating ionospheric delay variations*. According to Eq. (2), the l slant ionospheric delay variations $\hat{\nabla} I_1(t_{ji}, t_m)$ between the present observation epoch t_m $[t_m \in (t_{er1}, t_{er2})]$ and all ideal initial epochs t_{ji} in DI previously selected and stored in step (a) can be calculated.

(c) *Determining final slant ionospheric delay*. Combining the slant ionospheric delays $I_1(t_{ji})$ selected in step (a) with the corresponding slant ionospheric delay variations $\hat{\nabla} I_1(t_m, t_{ji})$ calculated in step (b), according to Eq. (3), the user can determine the slant ionospheric delays $\hat{I}_1(t_m)_{ji}$ $(j = 1, 2, \ldots, l)$ for the present observation epoch t_m. Then, k $\hat{I}_1(t_m)_j$ [which

Table 1. Analysis on accuracy of APR-I scheme under different conditions

k^a	Observation accuracy (σ_e) (m)																				
	0.30			0.50			0.70			1.00			1.20			1.50			2.00		
	σ_{q1}	σ_{q2}	σ_{q3}	σ_{q1}	σ_{q2}	σ_{q3}	σ_{q1}	σ_{q2}	σ_{q3}	σ_{q1}	σ_{q2}	σ_{q3}	σ_{q1}	σ_{q2}	σ_{q3}	σ_{q1}	σ_{q2}	σ_{q3}	σ_{q1}	σ_{q2}	σ_{q3}
1	0.21	0.37	0.54	0.35	0.46	0.61	0.5	0.58	0.70	0.71	0.77	0.87	0.85	0.90	0.98	1.06	1.10	1.17	1.41	1.45	1.50
2	0.18	0.28	0.40	0.31	0.37	0.47	0.43	0.48	0.56	0.61	0.65	0.71	0.73	0.76	0.82	0.92	0.94	0.98	1.22	1.24	1.27
3	0.17	0.24	0.34	0.29	0.34	0.41	0.40	0.44	0.50	0.58	0.60	0.65	0.69	0.71	0.75	0.87	0.88	0.91	1.15	1.17	1.19
4	0.17	0.23	0.30	0.28	0.32	0.38	0.39	0.42	0.46	0.56	0.58	0.61	0.67	0.69	0.72	0.84	0.85	0.88	1.12	1.13	1.15
5	0.16	0.21	0.28	0.27	0.31	0.35	0.38	0.41	0.44	0.55	0.56	0.59	0.66	0.67	0.69	0.82	0.83	0.85	1.10	1.10	1.12
6	0.16	0.20	0.26	0.27	0.30	0.34	0.38	0.40	0.43	0.54	0.55	0.58	0.65	0.66	0.68	0.81	0.82	0.84	1.08	1.09	1.10
7	0.16	0.20	0.25	0.27	0.29	0.33	0.37	0.39	0.42	0.53	0.55	0.57	0.64	0.65	0.67	0.80	0.81	0.83	1.07	1.08	1.09
8	0.16	0.19	0.24	0.27	0.29	0.32	0.37	0.39	0.41	0.53	0.54	0.56	0.64	0.64	0.66	0.80	0.80	0.81	1.06	1.07	1.08
9	0.16	0.19	0.23	0.26	0.28	0.31	0.37	0.38	0.40	0.53	0.54	0.55	0.63	0.64	0.65	0.79	0.80	0.81	1.05	1.06	1.07
10	0.16	0.18	0.22	0.26	0.28	0.31	0.37	0.38	0.40	0.52	0.53	0.55	0.63	0.64	0.65	0.79	0.79	0.80	1.05	1.05	1.06

[a] k is the number of initial epochs; σ_{q1}, σ_{q2} and σ_{q3} denote the initial accuracy σ_q equal to 0.0, 0.30 and 0.50 m, respectively

satisfies the condition of Eq. (4b) below] may be selected from $\hat{I}_1(t_m)_{ji}$

$$\left|\hat{I}_1(t_m)_j - \underset{1\leq j\leq l}{\mathrm{med}}\left[\hat{I}_1(t_m)_{ji}\right]\right| < G\cdot 1.483\cdot \underset{1\leq j\leq l}{\mathrm{med}}\left|\hat{I}_1(t_m)_{ji} - \underset{1\leq j\leq l}{\mathrm{med}}\left[\hat{I}_1(t_m)_{ji}\right]\right| \tag{4b}$$

where G is a robustness factor, which may be determined with the help of the user's experiences and measurement quality (the authors propose $G = 2$). Finally, the last ionospheric delay estimate $\bar{\hat{I}}_1(t_m)$ necessary to correct the pseudorange measurements for single-frequency GPS can be determined through the averaging of the above $\hat{I}_1(t_m)_j$ $(j = 1, 2, \ldots, k)$ according to

$$\bar{\hat{I}}_1(t_m) = \sum_{j=1}^{k} \hat{I}_1(t_m)_j/k \tag{5}$$

Assume that σ, σ_q, and σ_ε are the accuracies of the APR-I scheme result, initial absolute ionopheric delays and C/A code measurements, respectively. Then, according to Eq. (5) and the error propagation law

$$\sigma = \sqrt{\tfrac{1}{4}\sigma_\varepsilon^2 + \tfrac{1}{k}(\sigma_q^2 + \tfrac{1}{4}\sigma_\varepsilon^2)} = \sqrt{\tfrac{1}{4}(1 + \tfrac{1}{k})\sigma_\varepsilon^2 + \tfrac{1}{k}\sigma_q^2}$$
$$= \sqrt{\tfrac{1}{4}\sigma_\varepsilon^2 + \tfrac{1}{4k}\sigma_\varepsilon^2 + \tfrac{1}{k}\sigma_q^2} = \sqrt{\sigma_1^2 + \sigma_2^2 + \sigma_3^2} \tag{6}$$

From the above formula, one can see that the APR-I scheme accuracy σ consists of three components: $\sigma_1 = \frac{1}{2}\sigma_\varepsilon$, $\sigma_2 = \frac{1}{2}\sqrt{\frac{1}{k}}\sigma_\varepsilon$ and $\sigma_3 = \sqrt{\frac{1}{k}}\sigma_q$. Obviously, the size of σ_2 and σ_3 can be controlled by selecting more initial reckoning epochs. Then σ_1 will have the major effect on σ when APR-I is used to determine ionospheric delays. The accuracy of this scheme depends mainly on the accuracy of the C/A code observations. Hence, APR is most effective for the single-frequency users using narrow correlator L1 C/A code receivers.

4 Preliminary results and analyses

The accuracy of the APR-I scheme was estimated using Eq. (6). Table 1 shows the results of the accuracy of the ionospheric delay correction analysis for different initial epochs k and observation accuracy σ_ε (the average accuracy of ionospheric delay correction of the WAAS is about 0.30 m; Pullen et al. 1996). The results show that the best results are for initial reckoning epochs $k = 3$–5. This suggests that the APR-I scheme will not increase storage demand for receivers. From Eqs. (2) and (4), it can be seen that the size of the time interval between the initial reckoning epochs t_{ji} and the present observation t_m does not have any effect on σ. The equitable length of T can efficiently lessen, and even avoid, the effects from any system errors in $I_1(t_{ji})$ or $L_{DN1}(t_{ji})$. From Table 1, it can also be seen that the effects of σ_q on σ can also be controlled by selecting more initial reckoning epochs. $k = 5$ was selected for the next experiment.

In order to verify the ionospheric correction effectiveness of the APR-I scheme, five IGS stations (equipped with dual-frequency GPS receivers) in China were selected to constitute the reference stations of the experimental GPS network on Day304 of 1997 (SHAO station is selected as the user, and its C/A code and L1 phase measurements are used as single-frequency observations; other stations are WUHN, XIAN, LHSA, TAIW). Figures 3a and 3b illustrate the different

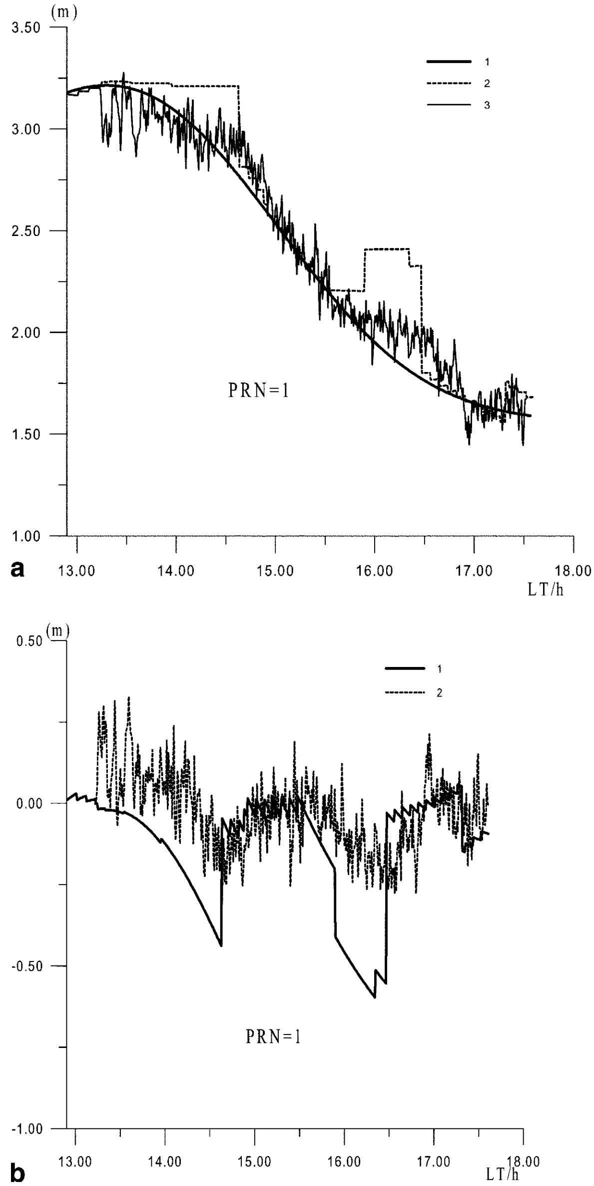

Fig. 3. **a** Comparison of ionospheric delays using the APR-I scheme and previous DIDCs when user can not obtain real time DIDCs. *1* The calculated IONs using dual frequency GPS data; *2* the estimated IONs using previous WAAS's DIDCs; *3* the estimated IONs using the APR-I scheme. **b** Comparison of ionospheric delay correction effectiveness using the APR-I scheme and previous WAAS's DIDCs when user can not obtain real time DIDCs from WAAS. *1* The correction effectiveness of WAAS's DIDCs; *2* the correction effectiveness of the APR-I scheme

correction results of the APR-I method and the DIDC previously received from the WAAS for satellite PRN = 1 when user has no real-time DIDC; that is, when DIDC cannot be normally broadcast (e.g. T1: 13:38–14:36/*h*, here *h* is local time), and when the DIDC cannot be received by users (e.g. T2: 15:34–16:28/*h*). From Figs. 3a and 3b, one can see that the effectiveness of the APR-I method is obviously better than using the previous DIDC values from the network during the periods T1 and T2. Figures 4a and 4b show the correction results of the APR-I method and the real-time DIDC during two periods (when short-timescale ionospheric disturbances have occurred), T3 (11:00–11:10/*h*) and T4 (13:32–13:42/*h*). From Figs. 4a and 4b, one can see that the effectiveness of the APR-I method is also better than that of the DIDC under those conditions. Figures 5a and 5b show a comparison of different correction results from the APR-I and the DIDC when there are gross errors in the DIDC. From Figs. 5a and 5b it can be seen that the APR-I has good robust performance in the presence of gross errors and can effectively avoid gross errors impacting on the generation of corrections for single-frequency receivers. However, it is impossible for the DIDC to account for gross errors.

Note that all the plots are for results determined according to step (2) of the APR procedure in Figs. 3–5, because the curves based on step (1) are the same as that

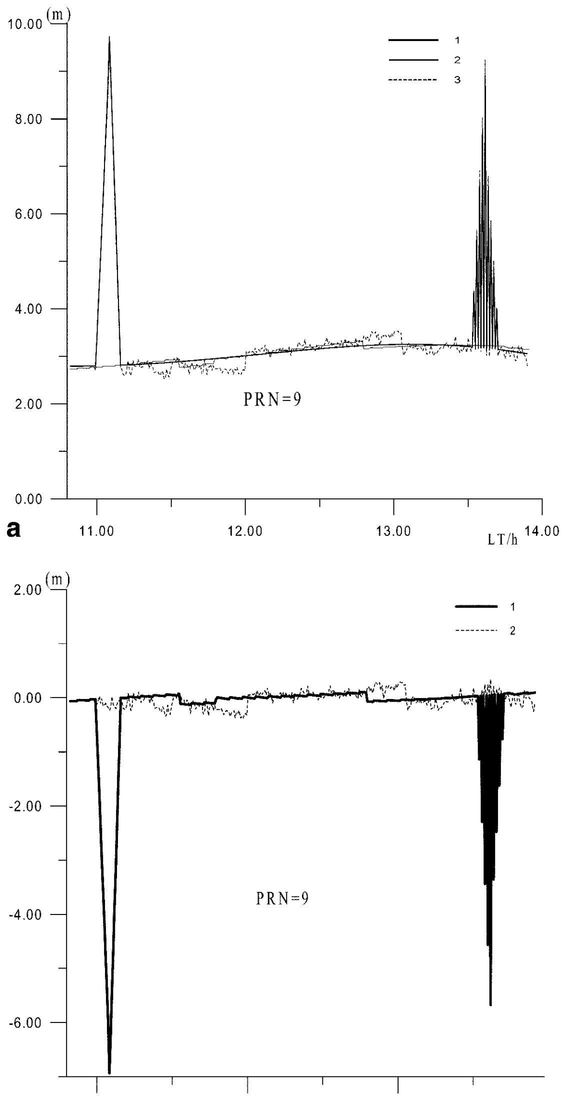

Fig. 4. **a** Comparison of the estimated ionospheric delays between the APR-I scheme and the DIDCs when short time scale ionospheric disturbances occur. *1* The calculated IONs using dual frequency GPS data; *2* the estimated IONs using real time DIDCs; *3* the estimated IONs using the APR-I scheme. **b** Comparison of correction effectiveness of ionospheric delays using the APR-I scheme and the DIDCs under short time scale ionospheric disturbance conditions. *1* The ION correction effectiveness from WAAS's DIDCs; *2* The ION correction effectiveness from the APR-I scheme

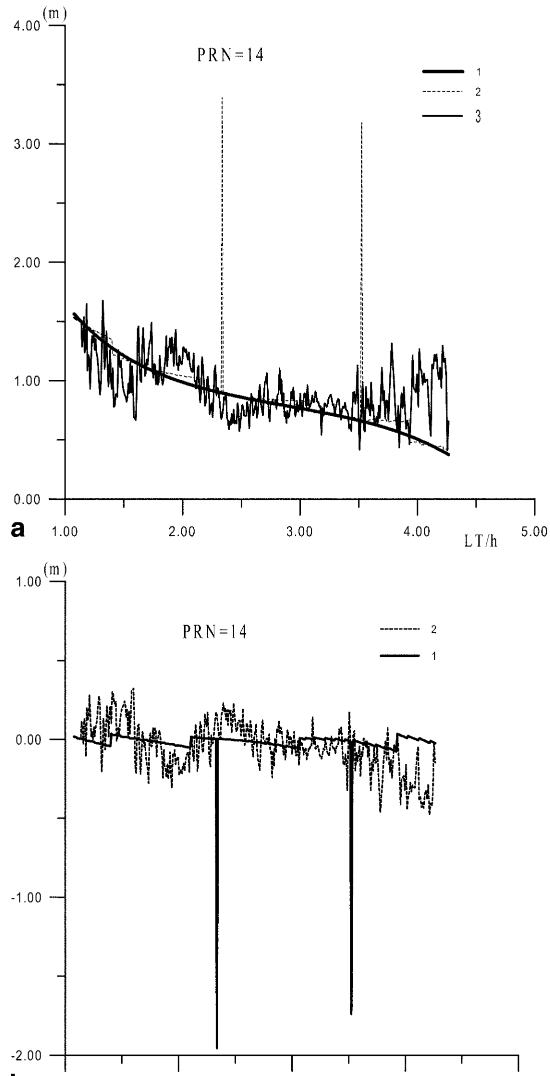

Fig. 5. **a** Comparison of the determined ionospheric delays using the APR-I scheme and WAAS's DIDCs when the DIDCs have gross errors. *1* The calculated IONs using dual frequency GPS data; *2* the estimated IONs using real time DIDCs; *3* the estimated IONs using the APR-I scheme. **b** Comparison of ionospheric delay correction effectiveness using the APR-I scheme and WAAS's DIDCs when the DIDCs have gross errors. *1* The ION correction effectiveness from WAAS's DIDCs; *2* the ION correction effectiveness from the APR-I scheme

of the DIDC. This also shows that step (1) ensures that the APR maintains good accuracy for the DIDC under normal conditions, while step (2) ensures that the APR has relatively better accuracy than the DIDC under abnormal conditions.

5 Conclusions and some suggestions

The experimental results discussed above show that the APR-I scheme for the correction of single-frequency GPS ionospheric delays presented in this paper not only retains the characteristic of high accuracy of the DIDC from the WAAS under normal ionospheric and reception conditions, but also has relatively better correction effectiveness under different, abnormal conditions. The implementation of this method need not change the present basic ionospheric delay correction algorithm of the WAAS. In addition, the APR-I method does not impose new demands on receiver hardware, and only requires a few improvements to receiver software. Hence it can be easily used by single-frequency GPS users. However, these are only preliminary results. More experiments and analyses, using various other GPS data sets under similar and abnormal ionospheric conditions, should be conducted. To further improve the accuracy and effectiveness of this scheme, more effective mathematical models for exact description of ionospheric variations need to be developed, filtering (see e.g. Goad 1990) should be introduced into the recurrence, and selection of initial reckoning epochs and corresponding subsidiary time periods must also be simplified. This ongoing research work will be useful in permitting an increase in the length of time periods for the broadcasting of the DIDC, in order to reduce the cost of the WAAS as well.

Acknowledgements. We would like to acknowledge the first author's supervisor, Prof. C.C. Tscherning, for his valuable suggestions, and Mr. Harry Goon and Prof. Zhu Wen Yiao for their help. We would also like to thank the Chinese Academy of Sciences (Grant N0.KZCX2-106) and the China Defense Committee of Science and Technology for their financial support. Special thanks should also be given to Prof. A. Dodson for handling the reviews, and Prof. C. Rizos and Prof. T. Moore for correcting the English grammar and making valuable comments.

References

Beutler G, Gurtner W, Hugentobler U, Rothacher M, Schildknecht T, Wild U (1988) Ionosphere and GPS processing techniques. Paper presented at 1988 Chapman Conf on the Use of GPS for Geodynamics, Fort Lauderdale

Campbell J, Maniatis T, Muller A, Vierbuchen J, Lohmar FJL (1986) On the generation of ionospheric refraction corrections for single frequency GPS measurements. Proc 4th Int Geod Symp Sat Pos, 28 April–2 May, Austin

Chao Y, Tsai Y, Walter T, Kee C, Enge P, Parkinson B (1995) An algorithm for inter-frequency bias calibration and application to WAAS ionosphere modeling. Proc ION GPS-95, Palm Springs, 12–15 September, pp 639–646

Conker R, Bakry M, El-Arini, Albertson T (1995) Development of real-time algorithms to estimate the ionospheric error bounds for WAAS*. Proc ION GPS-95, Palm Springs, 12–15 September, pp 1247–1258

Cohen C, Pervan B, Parkinson B (1992) Estimation of absolute ionospheric delay exclusively through single-frequency GPS measurements. Proc GPS-92, Albuquerque, 16–18 September, pp 325–330

Delikaraoglou D (1989) On the stochastic modelling of GPS ionospheric delays. Manuscr Geod 14: 100–109

Gao Y, McLellan J, Abousalem M (1996) A GPS positioning results using precise satellite ephemerides, clock corrections and ionospheric grid model with Jupiter™. Proc ION GPS-96, pp 25–34

Goad CC (1990) Optimal filtering of pseudoranges and phases from single-frequency GPS receivers. Navigation, J Inst Navig 37(3): 249–262

Georgiadou Y, Kleusberg A (1988) On the effect of ionospheric delay on geodetic relative GPS positioning. Manuscr Geod 13: 1–8

Georgiadiou Y (1994) Modelling the ionosphere for an active control network of GPS station. LGR series 7. Delft Geodetic Computing Centre, Delft

Henson JD, Collier EA (1986) Effects of the ionospheric on GPS relative geodesy. Proc IEEE PLANS'86, Las Vegas, 4–7 November

Ho M, Wilson BD, Mannucci AJ, Witer UJL, Yuan DN (1997) A comparative study of ionospheric total electron content measurements using global ionospheric maps of GPS, TOPEX radar, and the Bent model. Rad Sci 32(4): 1499–1512

Jin XX (1995) Prediction accuracy of GPS differential corrections and its change with latency. GPS Nieuwsbrief, 10th jaargang, no 2, November 1995, pp 1–6

Kloubuchar JA (1982) Ionospheric corrections for the single frequency user of the global positioning system. Proc Nat Telecommunication Symp, Galveston, 7–10 November

Li ZF, Schwarz KP (1996) Multiscale estimation of the ionospheric effect from single frequency GPS receiver data. IEEE Position Location and Navigation Symp, Atlantic City, April, pp 620–625

Lin LS, Rizos C, Wang YJ (1996) Real-time estimation of ionospheric time delays using GPS. Int Conf GPS, Taipei, 12–13 June, pp 117–127

Ou JK (1996) Atmosphere and its effects on GPS surveying. LGR series 14. Delft Geodetic Computing Centre, Delft

Pullen PS, Chao YC, Enge PK (1996) Effects of local ionospheric anomalies on navigation performance and integrity using WAAS. IEEE Position Location and Navigation Symp, Atlantic City, April, pp 574–581

Qiu W, Lachapelle G, Cannon ME (1995) Ionospheric effect modelling for single frequency GPS users. Manuscr Geod 20: 96–109

Sardon E, Rius A, Zarraoa N (1994) Ionospheric calibration of single frequency VLBI and GPS observations using dual GPS data. Bull Geod 68: 230–235

Wang YJ, Wilkinson P, Caruana J, Wu J (1996) Real-time ionospheric TEC monitoring using GPS. Proc 10th Space Engineering Symp, Canberra, 27–29 March, pp 101–111

Wang YJ, Wilkinson P (1997) Preliminary results of using GPS to observe ionospheric scintillation at Vanimo PNG. Presented at USAF workshop on Space Weather Effects on Propagation of Navigation and Communication Signals, Washington, DC, 22–24 October

Wild U, Beutler G, Faukhauser S, Gurtner W (1990) Stochastic properties of the ionosphere estimated from GPS observations. GPS'90, Ottawa

Yuan YB, Ou JK (1999) The effects of instrumental bias in GPS observation on determining ionospheric delays and the methods of its calibration. Acta Geod Cartogr Sin 28(2): 110–114